Contents lists available at ScienceDirect

Geoderma

journal homepage: www.elsevier.com/locate/geoderma



¹⁴C mean residence time and its relationship with thermal stability and molecular composition of soil organic matter: A case study of deciduous and coniferous forest types



Tsutomu Ohno^a,*, Katherine A. Heckman^b, Alain F. Plante^c, Ivan J. Fernandez^d, Thomas B. Parr^e

- a School of Food and Agriculture, University of Maine, Orono, ME 04469, USA
- ^b USDA Forest Service, Northern Research Station, Houghton, MI 49931, USA
- ^c Department of Earth and Environmental Sciences, University of Pennsylvania, Philadelphia, PA 19104, USA
- d School of Forest Resources, University of Maine, Orono, ME 04469, USA
- e Department of Biology, University of Oklahoma, Norman, OK 73019, USA

ARTICLE INFO

Keywords: Soil organic carbon Carbon sequestration Soil minerals Radiocarbon dating Thermal analysis Ultrahigh resolution mass spectrometry

ABSTRACT

Soil organic matter (SOM) plays a critical role in the global terrestrial carbon cycle, and a better understanding of soil processes involved in SOM stability is essential to determine how projected climate-driven changes in soil processes will influence carbon dynamics. We used 14C signature, analytical thermal analysis, and ultrahigh resolution mass spectrometry to determine the influence of deciduous and coniferous forest vegetation type and soil depth on the stability of soil C. The 14C mean residence time (MRT) of the illuvial B horizon soils averaged 1350 years for the deciduous soils and 795 years for the coniferous soils. The difference of MRT between mineral soils by forest type may be due to the saturation of extractable Fe and Al minerals binding sites by SOM in the coniferous soils, allowing greater transport of modern SOM from the O horizon down the soil profile, as compared with the non-saturated minerals in the deciduous soil profile. The molecular mass distribution of the deciduous water-extractable aromatic SOM fraction was shifted to a lower mass range in the lower portion of B horizon soil compared with the upper portion, indicating preferential sorption of the higher mass aromatic fraction. The shift in the mass distribution of the aromatic fraction in the coniferous soil was much less than in the deciduous soil, which supports the view that the extractable metal minerals had reached saturation. We conclude that greater transport of modern O horizon SOM to the lower mineral B horizons in the coniferous soil profile resulted in its radiocarbon enrichment and shorter estimated MRT. Our findings highlight the importance of forest vegetation type, soil depth and transport mechanisms on SOM stability, and suggest important ecological implications for changes in forest composition on the terrestrial C cycle.

1. Introduction

Soil organic matter (SOM) is a complex, heterogeneous mixture of compounds that is produced predominately by the continuous microbial processing of plant biomass inputs into molecules of lower mass (Lehmann and Kleber, 2015). Globally, soils to a depth of one meter deliver a critical ecosystem service by storing the largest pool of terrestrial C, which is estimated to be 1461 Pg of C (Scharlemann et al., 2014). SOM stability, defined as its resistance to microbial decomposition and resulting in long mean residence times (MRT), is of great interest because of the uncertainty in the fate of SOM in response to climate change feedback forces (Peltre et al., 2013). A new paradigm proposes that SOM stability results from its physico-chemical and biological interactions with its immediate environment (Schmidt et al., 2011). Transport of dissolved organic matter (DOM) components down a soil profile combined with microbial recycling has been proposed as a mechanism responsible for older DOM components in subsoil horizons (Kaiser and Kalbitz, 2012). In this conceptual model, the plant-derived DOM from the soil surface preferentially adsorbs to the reactive sites on the mineral surface, exchanging more weakly bound DOM molecules into soil solution, to be transported further down the soil profile. The adsorbed SOM ages as its decomposition rate is reduced in its adsorbed state. In support of this model, a simulation study has shown that both adsorptive stabilization and repeated microbial processing of SOM are the dominant mechanisms leading to the persistence of SOM (Ahrens et al., 2015).

Numerous physical and chemical approaches have been used to investigate the stability of SOM. The 14C radioisotope has a half-life of

^{*} Corresponding author. E-mail address: ohno@maine.edu (T. Ohno).

T. Ohno et al. Geoderma 308 (2017) 1–8

5730 years and its content in soils can provide an estimated SOM MRT, which relates to its stability (Trumbore et al., 1989). A meta-analysis of 122 soil radiocarbon profiles found decreasing Δ^{14} C values, which indicate greater SOM average age, with increasing soil depth in nearly all profiles (Mathieu et al., 2015). The statistical analysis of the 122 profiles indicated that a model with climate, location, vegetation, and soil type can predict SOM Δ^{14} C with 85% accuracy. A simulation study (Ahrens et al., 2015) has shown that a model that includes sorption, transport, and microbial processes can predict the increasing radiocarbon average age of SOM with greater soil depth without invoking a pool of soil carbon with very slow decomposition kinetics. Thermal analysis methods, such as scanning calorimetry and CO2-evolved gas analysis (CO2-EGA) during ramped combustion of whole soils, provides information on the thermal energy needed to oxidize SOM to CO2, which reflects the energy required to oxidize the SOM itself, as well as the energy needed to break any existing bonds between SOM and mineral functional groups (Peltre et al., 2013). Although the decomposition of SOM is a biologically driven process in soils, strong statistical relationships between biological and thermal measurements of SOM stability suggest that thermal methods can be used to study SOM stability (Plante et al., 2011; Peltre et al., 2013). The chemical characterization of SOM has also advanced in the past decade with the use of electrospray ultrahigh resolution mass spectrometry, which allows detection of thousands of individual SOM components (Sleighter and Hatcher, 2007). The ability to determine molecular mass to five decimal places makes it possible to unambiguously assign empirical elemental formulas for most of the resolved mass peaks based on the atomic masses of the constituent atoms.

A previous study conducted to examine the influence of forest type and soil depth on the chemical characteristics of the water-extractable organic matter (WEOM) fraction found that in comparing the upper 0-5 cm versus lower 25-50 cm B layer soils, the relative abundance of lipids and carbohydrate components significantly increased, while the condensed aromatic and tannin components decreased for the deciduous forest soils, but no changes were observed for the coniferous forest soils (Ohno et al., 2014). Our aim with this further study was to gain a better understanding of processes controlling SOM stability of soils under different forest vegetation. This will be critical to more fully understand the implications of projected climate driven changes in forest type on SOM stability. Specifically, we expand upon the previous study conducted at the Bear Brook Watershed in Maine (Ohno et al., 2014) by determining the stability of bulk SOM using 14C abundance and thermal analysis. Here, we also add the characterization of the chemical composition of pyrophosphate-extractable organic matter (PPEOM) fraction using ultrahigh resolution mass spectrometry to clarify how SOM chemical composition affects its stability.

2. Methods

2.1. Field site and soil analysis

The field site is the reference watershed located at the Bear Brook Watershed in Maine (BBWM, $44^{\circ}52'$ N, $68^{\circ}06'$ W), USA (Norton et al., 1999). The watershed is composed of 65–70 year-old mixed deciduous stands with American beech (Fagus grandifolia Ehrh.), yellow birch (Betula alleghaniensis Britton), red maple (Acer rubrum L.), and sugar maple (Acer saccharum Marshall) in the lower elevations (~250–370 m), and 100 + year-old coniferous stands dominated by red spruce (Picea rubens Sarg.) in the higher elevations (~370–450 m). Deciduous stands are believed to have been in deciduous and mixed wood forest since the early 1800s, and coniferous stands have been in a continuous coniferous forest type. Deciduous and coniferous sampling sites are approximately 200 ± 50 m apart. The coniferous stand is in the upper portion of our watershed, which transitions with decreasing elevation into mixed forest type, below which is the deciduous forest type sampled here. So there is both distance and a transition stand in

between the deciduous and coniferous stands sampled for this study. The forest floor in conifer stands (mor-like type) is three times as thick as that in deciduous stands (moder-like type). Soils are coarse-loamy, isotic, frigid, Typic Haplorthods formed from till (~1 m thick) primarily over a quartzite and gneiss bedrock. Additional details about the experimental BBWM watershed can be found in Norton (1999).

Two different BBWM soil sets were used in this study. Soils used in the ¹⁴C dating; water-, pyrophosphate-, and oxalate-extraction based chemical characterizations; and ultrahigh resolution mass spectrometry analyses were sampled in 2012 from a single pedon (~70 × 70 cm wide) in each of the deciduous and coniferous forest types to provide highly resolved soil depth information. The soils were manually sampled with a knife from one side of the pedon to obtain a grab sample with proportional representation throughout the horizon. B horizons were sampled in 5 cm increments from the top of the B horizon (= 0 cm depth for the B horizon), where there is an abrupt boundary with the E horizon, to a depth of 25 cm followed by a sample from a depth of 25-50 cm. Soils for the thermal characterization were also sampled in 2012 from three replicate quantitative pedons sampled at 0-5 cm, 5-25 cm, and 25-50 cm (or to the top of the C-horizon). All soil samples were placed in plastic bags and kept cold in coolers during the field sampling. After transport to the laboratory, they were refrigerated for up to 48 h before further processing. All soil samples were sieved field moist through a 2-mm sieve for mineral horizons or a 6-mm sieve for the organic horizons, then stored in paper bags to air-dry at room temperature. Samples were subsequently stored in plastic bags for archiving.

Soil total C and N were determined using a LECO CN-2000 analyzer on ground samples (SPEX 8000 ball mill). Soils were extracted with a 0.2 ammonium oxalate solution at pH 3 (Iyengar et al., 1994), and the Al and Fe contents of the extracts were measured by inductively-coupled plasma-atomic emission spectroscopy (ICP-OES). Oxalate-extractable Fe and Al pools were assumed to represent metals from amorphous phases and poorly crystalline minerals (Pansu and Gautheyrou, 2006). SOM extracted by pyrophosphate was assumed to be sourced from amorphous organo-metal complexes (Schnitzer and Schuppli, 1989; Wagai et al., 2013). Root data (unpublished) were obtained from BBWM soil samples collected in 2010 from long-term quantitative pedon sampling locations used in 2006 by SanClements et al. (2010). Roots were manually picked from both fine (< 6 mm) and coarse (≥ 6 mm) fresh soil samples and summed for an estimate of root biomass in each forest stand. Roots were dried at 70 °C prior to determination root dry biomass.

2.2. 14C analysis

Soil samples were graphitized in preparation for 14C abundance measurement at the USDA Carbon, Water & Soils Research Lab in Houghton, Michigan. Samples were dried, weighed into quartz tubes and sealed under vacuum. Samples were combusted at 900 °C for 6 h with cupric oxide (CuO) and silver (Ag) in sealed quartz test tubes to form CO2 gas. The CO2 was then reduced to graphite through heating at 570 °C in the presence of hydrogen (H₂) gas and an iron (Fe) catalyst (Vogel et al., 1987). Graphite targets were then analyzed for radiocarbon abundance (Davis et al., 1990) and corrected for mass-dependent fractionation using measured $\delta^{13}\text{C}$ values according to Stuiver and Polach (1977). The year of measurement was 2015, and data are given Δ^{14} C. The Δ^{14} C values were used to calculate estimated mean residence times (MRT) for bulk soil C at different depths in the soil (Trumbore, 1993; Torn et al., 2009). The model assumes steady state conditions and does not account for lag times associated with movement of C among depths or pools and therefore estimated values are likely overestimates. MRT values are presented to allow for ease of interpretation and comparison among depths and sites.

2.3. Analytical thermal analysis

Differential scanning calorimetry (DSC) and coupled CO2-evolved gas analysis (CO2-EGA) were performed as described by Peltre et al. (2013). Briefly, ramped combustion was performed using a Netzsch STA 409PC Luxx coupled to a LI-840A CO₂/H₂O IRGA. Samples were weighed to obtain approximately 1 mg C, with a maximum of 50 mg soil to avoid excess thermal disequilibrium. Samples were heated from ambient (\sim 25 °C) to 800 °C at 10 °C min⁻¹, in an atmosphere of CO₂-free air flowing at 30 mL min⁻¹ and N₂ protective gas flowing at 10 mL min⁻¹. DSC thermograms were baseline corrected for the region between 120 and 800 °C using the non-parametric baseline fitting function of Peakfit (Systat Software). The net exothermic energy content (mJ g⁻¹ soil) was determined by integrating the DSC thermogram, and net energy density (J mg-1C) was calculated as energy content divided by the sample C concentration. The temperatures at which half of the energy was released (DSC-T50) and half of the CO2 was evolved (CO₂-T₅₀) were also calculated. These temperatures are indices of the amount of energy inputs required for the combustion of the organic matter, and are therefore indices of overall thermal SOM stability. Net exo energy content and density are indices of the amount of energy stored in SOM and released during combustion, over and above any endothermic reactions from the mineral matrix.

2.4. Ultrahigh resolution mass spectrometry analysis

The WEOM fraction of the soil was extracted with deionized distilled water at a 1:10 soil: deionized-water ratio for 30 min. Pyrophosphate-extractable organic matter (PPEOM) was extracted by adding 25 mL of 0.125 M sodium pyrophosphate solution to 3 g of soil, and shaking for 16 h. Both extracts were centrifuged, and vacuum filtered through a 0.4 μm polycarbonate filter before the dissolved organic carbon (DOC) concentration was measured using a Shimadzu 5000 TOC Analyzer. The WEOM and PPEOM extracts were processed through Agilent PPL solid-phase extraction cartridges to desalt the extract for subsequent electrospray ionization FT-ICR-MS (Dittmar et al., 2008). The extracts were characterized using negative ion mode electrospray ionization with a 12 T Bruker Daltonics Apex Qe FT-ICR-MS instrument at the COSMIC facility at Old Dominion University. To increase the ionization efficiency, ammonium hydroxide was added immediately prior to ESI to raise the pH to 8. Samples were introduced by a syringe pump providing an infusion rate of 120 $\mu L \, h^{-1}$ and analyzed in negative ion mode with electrospray voltages optimized for each sample. Ions (in the range of $200-2000 \, m/z$) were accumulated in a hexapole for 1.0 s before being transferred to the ICR cell. Exactly 300 transients, collected with a 4 MWord time domain, were added for a total run time of ~30 min. The summed free induction decay signal was zero-filled once and Sine-Bell apodized prior to fast Fourier transformation and magnitude calculation using the Bruker Daltonics Data Analysis software. Prior to data analysis, all samples were externally calibrated with a polyethylene glycol standard and internally calibrated with naturally present fatty acids within the sample.

For assignments of molecular formulas, m/z values with a signal to noise ratio above 5 were assigned using the formula extension approach (Kujawinski and Behn, 2006). The modified aromaticity index (AI_{mod}) (1 + C - 1/2O - S - 1/2H)/(C - 1/2H)calculated as 2O - S - N - P) and the double bond equivalents (DBE) were calculated as 1 + 1/2(2C - H + N + P) (Koch and Dittmar, 2006). A MA-TLAB script was used to parse the assigned formulas into the appropriate van Krevelen space, which consisted of four discrete regions (Seidel et al., 2014): 1) condensed aromatic molecules (AI_{mod} > 0.66); 2) aromatic molecules (0.66 \geq AI_{mod} > 0.50); 3) highly unsaturated molecules (AI_{mod} \leq 0.50 and H/C < 1.5); and 4) aliphatic molecules $(2.0 > H/C \ge 1.5)$. The cumulative mass profile function was produced by binning the mass spectrometry peak intensities and dividing by total intensity into 10-Da increments between 220 and 800 Da. The plots have reference lines at the 0.5 cumulative sum, which represent the mass at which half of the total peak intensity is accumulated, and the 600-Da threshold for strong WEOM binding indicated by an AFM study (Chassé and Ohno, 2016). A Venn analysis was conducted to determine the chemical properties of marker WEOM molecules uniquely present in the 0–10, 10–20, and 20–50 cm soil depths. Further post-processing details can be found elsewhere (Ohno and Ohno, 2013).

2.5. Statistical analysis

The radiocarbon, extractive chemical characterization, and ultrahigh resolution mass spectrometry data for this study are based on samples from a single pedon in each forest type that was sampled by soil horizon and depth increment. Each pedon is referred to as a deciduous and coniferous soil indicative of its origin without assumption as to its representativeness for the larger landscape. The lack of replication within forest types was to allow available resources to be focused on the intense chemical analysis of soil from each pedon as a case study. For the properties investigated, there also appears to be relatively low variability under a given condition as shown below by two means of appraisal.

The low variability of uppermost 0-5 cm B-layer organic matter chemical composition is demonstrated by the tight overlapping of the van Krevelen diagram of soils from three replicate sampling sites within the deciduous forest type stand in 2006 (Supplementary Fig. S1). The 95% confidence error ellipse defines the van Krevelen space that contains 95% of the data points assuming that the data follows a Gaussian distribution. The region common to all three ellipses (1.38 arbitrary units) accounts for 82% of the region total area encompassed by the three ellipses (1.69 arbitrary units) indicating relatively low variability of the chemical composition across the forest type stands. For clarity, the figure displays only 500 randomly selected data points for each replicate. However the ellipses shown are calculated with the complete data set of peaks for each of the replicates. The replicated thermal chemical characterization of the bulk soil samples (this study) were statistically analyzed using analysis of variance (ANOVA). The coefficient of variation for the soil energy density and CO2-T50 parameters were 6.2% (range of 2.9-8.9%) and 2.7% (0.6-4.7%), respectively, averaged over the 3 soil depths in the two forest type stands. This also shows that the bulk soil chemical parameters have relatively low variability, and suggests that the single pedon based 14C data can be used with confidence.

Correlation analysis was used to relate SOM MRT to assigned formulas of the PPEOM fraction (Singer et al., 2012; Seidel et al., 2014). First, the assigned formulas for the mineral horizon soils for each forest type separately were merged into a single matrix by their formula stoichiometry and abundance intensity using a R script. Then, Spearman rank correlations were calculated to relate the abundance of individual assigned formulas to SOM MRT for formulas present in all or all but one B horizon soil.

3. Results and discussion

3.1. Total C, extractable C, and radiocarbon content

In this study, we focus our discussion on the illuvial B horizon soils because in forested Spodosols they are the mineral horizons that accumulate the most SOM. The B horizon total soil C averaged over each of the sampling depths was 2.5 greater in the coniferous soils than in the deciduous soils. Similarly, the pyrophosphate-extractable organic matter (PPEOM) was 2.3 greater and the water-extractable organic matter (WEOM) was 7.6 times greater in the coniferous soils as compared to the deciduous soils (Table 1). The WEOM proportion averaged $2.1 \pm 1.0\%$ and $5.7 \pm 1.7\%$ of the total soil C for the deciduous and coniferous forest stands, respectively (Table 1). WEOM represents the most labile form of SOM, and presumably the fraction most directly

Table 1
Selected soil chemical properties of the deciduous and coniferous forest type soils collected at depth increments.

Soil horizon/ depth	Total soil C (g kg ⁻¹ soil)	Pyrophosphate extractable C (g kg ⁻¹ soil)	Water- extractable C (g kg ⁻¹ soil)	Oxalate extractable Al + Fe (mmol kg ⁻¹ soil)
Deciduous				
0	438	5.7	13.5	85
E	18	3.0	1.54	43
B 0-5 cm	28	14.2	1.07	276
B 5-10 cm	26	14.3	0.64	320
B 10-15 cm	30	18.6	0.57	449
B 15-20 cm	27	16.9	0.37	498
B 20-25 cm	34	21.7	0.49	508
B 25-50 cm	30	19.4	0.42	511
Coniferous				
0	493	6.2	29.4	71
E	13	2.1	2.08	35
B 0-5 cm	70	38.0	4.12	801
B 5-10 cm	66	35.1	4.43	746
B 10-15 cm	73	41.0	5.10	825
B 15-20 cm	68	36.1	4.83	595
B 20-25 cm	79	42.5	3.83	830
B 25-50 cm	81	43.8	2.20	1160

involved in chemical reactions such as complexation with dissolved ions and sorption to surfaces (Zsolnay, 2003). The pyrophosphate extraction represented 59.8 \pm 5.6% and 54.1 \pm 1.1% of the total soil C in the deciduous and coniferous B horizon soils, respectively (Table 1). The PPEOM consists of SOM desorbed through a solubilization and peptization process and likely consists of SOM complexed by metals and precipitated onto mineral surfaces (Schnitzer and Schuppli, 1989).

The deciduous and coniferous SOM MRT depth profile patterns also differed between the two forest type soils (Fig. 1). The deciduous forest SOM steadily increased in MRT with greater soil depth from 233 years for the surface O horizon to 1560 years for the B 15–20 cm soil depth, and the MRT remained approximately the same at the lower depths. In contrast, the coniferous forest SOM displayed a different pattern with surface O horizon MRT of 293 years, increasing to 1030 years for the E horizon, and remaining about 740 years for the B 0–25 cm layer before increasing again to 1100 years for the lowest B 25–50 cm layer. There

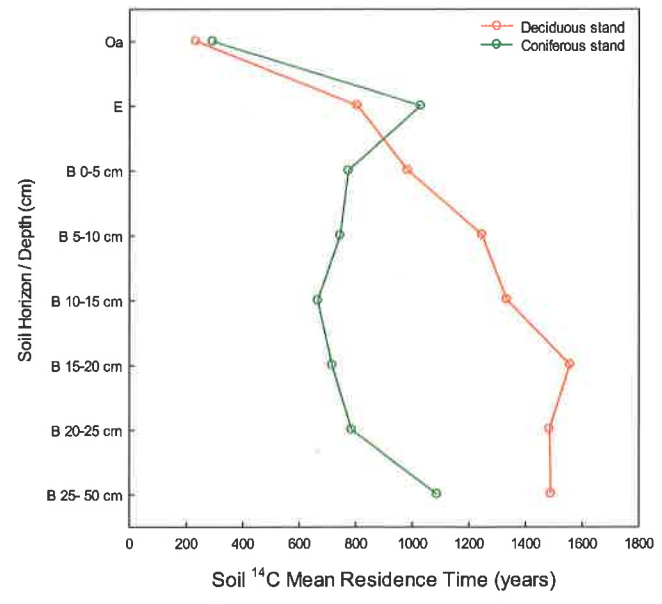


Fig. 1. Soil organic matter $^{14}\mathrm{C}$ mean residence time as a function soil horizon/depth for the deciduous and coniferous soils.

was a strong forest type effect with the MRT of deciduous B horizons soils being 1350 \pm 212 years (averaged over the six B horizon sampling depths), which was significantly (p=0.001) longer than the 795 \pm 149 years for the coniferous B horizons soils.

3.2. Role of amorphous Fe and Al minerals on soil C storage and stability

The growing acceptance that SOM stability is controlled by physical and chemical interactions among mineral phases and biological activity (Schmidt et al., 2011) emphasizes the role of amorphous metal phases and poorly crystalline Fe and Al minerals as critical factors in determining SOM stability. The [Fe + Al] averaged 826 \pm 185,103 mmol kg $^{-1}$ soil for the six coniferous B horizon soils and 427 \pm 103 mmol kg $^{-1}$ soil for the six deciduous B horizon soils (Table 1). The higher amorphous and poorly crystalline Fe and Al concentrations in the coniferous soils are likely due to more intensive podsolization because of the higher acidic inputs from the conifer litter. One possible mechanism for the ¹⁴C enrichment in the coniferous forest soils may be due to a greater fraction of the modern O horizon SOM being transported to the lower mineral horizons because of SOM saturation of amorphous Fe and Al sorption sites in the coniferous forest soils. This would be consistent with reported consistently higher concentrations of dissolved organic carbon (DOC) in coniferous stand soil solutions compared with deciduous stand soil solutions (Fernandez et al., 1999).

There was an increase in PPEOM content with increasing extractable Al and Fe loading (Fig. 2). The slopes of the regression representing the loading rates were 24.7 \pm 7.2 mg C mmol $^{-1}$ [Fe + Al] for the deciduous and 15.2 \pm 5.8 mg C mmol $^{-1}$ [Fe + Al] for the coniferous B horizon soils. The slopes of the linear regression fits representing the loading rates were not significantly (p=0.33) different. Additionally, the WEOM content (Table 1) for the coniferous B horizon soils was significantly higher (p=0.001) with an average of 4.1 \pm 1.0 g kg $^{-1}$ soil as compared to 0.59 \pm 0.25 g kg $^{-1}$ soil for the deciduous soils. The lower WEOM content of deciduous soils is likely due to the ability of the amorphous Fe and Al phases and poorly crystalline Fe and Al minerals to adsorb the DOM that is being translocated through the soil mineral horizons.

While the above evidence supports the interpretation that metaland mineral-associated SOM may have reached adsorptive saturation in the coniferous soils, allowing younger SOM to be translocated more easily to the lower mineral horizons, other explanations are possible. Clearly, larger inputs of modern carbon in the coniferous stand mineral

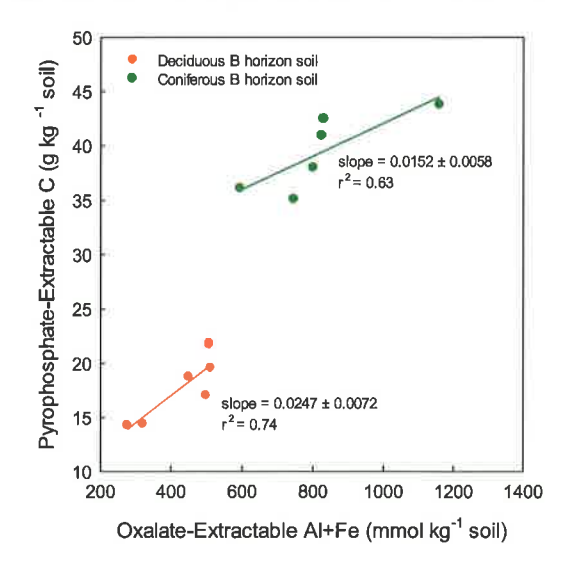


Fig. 2. Adsorbed pyrophosphate-extractable organic matter as a function of Fe and Al short range-ordered mineral content for the deciduous and coniferous soils.

Table 2Mean total root biomass of the deciduous and coniferous forest type soils collected at depth increments in the reference East Bear watershed at Bear Brook Watershed in Maine.

Soil horizon/depth	Mean total roots (kg ha ⁻¹)	Standard deviation		
Deciduous				
0	11,100	13,600	4300	10
B 0-5 cm	2230	949	300	10
B 5-25 cm	4670	3520	1110	10
B 25-50 cm	1700	916	648	2
B 25 cm-C	1100	1050	471	5
B 50 cm-C	112	66	46	2
С	2160	4240	1730	6
Sum total roots	23,100			
Coniferous				
0	10,400	7120	22,501	10
B 0-5 cm	1270	1300	410	10
B 5-25 cm	4640	2740	913	9
B 25-50 cm	3560	4420	2550	3
B 25 cm-C	695	562	229	6
B 50 cm-C	243	157	111	2
С	3510	6210	2540	6
Sum total roots	24,300			

soils may bias the total SOM to a lower MRT value. One possibility is that the greater organic matter content in the coniferous stand (SanClements et al., 2010), including a much thicker forest floor, results in a younger SOM as part of the age signal. Parent materials are the same for both deciduous and coniferous stands, resulting in similar physical properties for mineral soils. However, coniferous stands had approximately twice the mass of fine fraction O horizon materials compared to deciduous stands, and slightly lower densities (SanClements et al., 2010). Another factor may be differences in root biomass between the two forest type stands. However, total root biomass within the two stands was similar (Table 2), making differences in root-derived input of modern C less likely as a cause of dissimilarity in the MRT pattern observed in the mineral soil horizons. These results support our explanation of soil C adsorptive saturation as a mechanism for the difference in SOM stability and turnover in the two forest types.

3.3. Thermal analysis of soils

There was no significant effect of soil B-horizon depth on the SOM energy density in either forest type soil (p>0.78) (Table 3). However, the average B horizon energy density was $28.9\pm1.7~\rm J~mg^{-1}$ soil C for the deciduous type soil and $31.0\pm1.3~\rm J~mg^{-1}$ soil C for the coniferous forest type soil, which was significantly different (p>0.045). The traditional interpretation of this observation would be that SOM decomposition is occurring faster in the deciduous stand leaving behind organic matter with reduced caloric content, which some have termed low "quality" (Minderman, 1968). However, recent studies have shown that organic matter quality may remain constant or increase with decomposition (Rovira et al., 2008).

Inorganic materials can contribute endothermic and exothermic

Table 3 Soil organic matter energy density and the temperature at which half of the ${\rm CO_2}$ was evolved as a function of soil B horizon depth for the deciduous and coniferous soils. Values presented are mean \pm standard deviation, n=3. Energy density is the integral of the differential scanning calorimetry signal divided by the thermogravimetric mass loss of the organic matter in the exothermic region.

Soil horizon/depth	Energy density	(J mg ⁻¹ soil C)	CO ₂ -T ₅₀ (°C)		
layer	Deciduous	Coniferous	Deciduous	Coniferous	
B 0-5 cm	30.9 ± 1.5	29.7 ± 2.5	351 ± 10	324 ± 9	
B 5-25 cm	28.1 ± 1.8	30.9 ± 2.8	364 ± 2	323 ± 15	
B 25 + cm	27.8 ± 0.8	32.4 ± 1.9	359 ± 1	324 ± 13	

reactions, which can affect the interpretation of DSC characterization of SOM. The advantage of CO_2 -EGA over DSC is that the former is unaffected by mineral thermal reactions such as the dehydroxylation of minerals (Karathanasis and Harris, 1994; Fernández et al., 2012; Song and Boily, 2016). Inorganic materials can contribute to the heat flux measured in thermogravimetric analysis, which may affect the interpretation of the energy density parameter (Fernández et al., 2012). The region around 300 to 350 °C has been attributed to the combustion of carbohydrates and other aliphatic SOM molecules; while the region around 400 to 450 °C has been attributed to combustion of aromatic and polyphenolic compounds; and the > 500 °C region to the combustion of polycondensed aromatic molecules (Fernández et al., 2012). The CO_2 -EGA thermograms of the deciduous and coniferous soils are qualitatively similar (Supplementary Fig. S2) with B horizon SOM clustering together.

The $\rm CO_2$ - $\rm T_{50}$, defined as the temperature at which 50% of the $\rm CO_2$ is evolved, was 358 \pm 6 °C for the deciduous forest stand and 336 \pm 2 °C for the coniferous forest type B horizon SOM, which were statistically (p=0.007) different (Table 3). Energy density and $\rm CO_2$ - $\rm T_{50}$ (Table 3) data are consistent with the hypothesis that greater SOM saturation leads to increased transport of the younger SOM to deeper horizons in the coniferous type soil as the mechanism of the observed stability differences. Additionally, higher $\rm CO_2$ - $\rm T_{50}$ values have been attributed to lower surface coverage of C in soils (Peltre et al., 2013). Thus, the higher $\rm CO_2$ - $\rm T_{50}$ values in the deciduous forest type B horizon soils may indicate lower surface coverage (saturation) of SOM for the deciduous soils as compared with the coniferous soils.

3.4. FT-ICR-MS characterization of WEOM

An earlier BBWM study that included WEOM from deciduous and coniferous soil profiles showed that the aromatic and N-containing aliphatic molecules were positively correlated with the binding force between the WEOM and goethite-functionalized atomic force microscopy (AFM) tips (Chassé et al., 2015). In a separate AFM study, it was shown that aromatic WEOM components > 600 Da were able to compete with orthophosphate for binding sites on goethite (Chassé and Ohno, 2016). These two AFM studies indicate that high molecular mass aromatic and N-containing aliphatic components of WEOM are preferentially adsorbed to metal (oxy)hydroxide minerals in nano-scale laboratory studies.

If our hypothesis that the coniferous forest type SOM is ¹⁴C enriched because the amorphous metal (oxy)hydroxide minerals have reached adsorptive saturation allowing younger SOM to reach the deeper soil depths with less adsorptive retention is correct, then we should see less change in the molecular mass profiles of the aromatic WEOM fraction with depth in the coniferous stand soil as compared with the deciduous stand soil. For the deciduous forest soils, the cumulative sum distribution shifts to low masses with the centroid masses less at the B 25-50 cm layer (435 Da) as compared to the B 0-5 cm layer (510 Da) for the aromatic molecules (Fig. 3A). For the coniferous forest soils, the cumulative plot distribution shifts only slightly at depth with the centroid mass contrasts for the aromatic being 495 for the 0-5 cm B layer and 485 Da for the 25-50 cm layer (Fig. 3B). The same trends are seen in the cumulative distribution over 600 Da data where 26% of the deciduous SOM aromatic intensity is over 600 Da in the B 0-5 cm layer, but only 5% for the B 25-50 cm layer suggesting that the > 600-Da aromatic components are being preferentially adsorbed (Fig. 3A & B). The coniferous SOM aromatic intensities were both 24%, indicating that there was no preferential adsorption of the > 600-Da aromatic molecules.

The H/C ratio and the modified aromaticity index of the marker WEOM molecules identified using a Venn analysis of the assigned formulas decreases steadily with depth for the deciduous stand soils, indicating the preferential adsorption of the aromatic WEOM molecules (Table 4). The decrease in O/C ratio is likely to be the result of

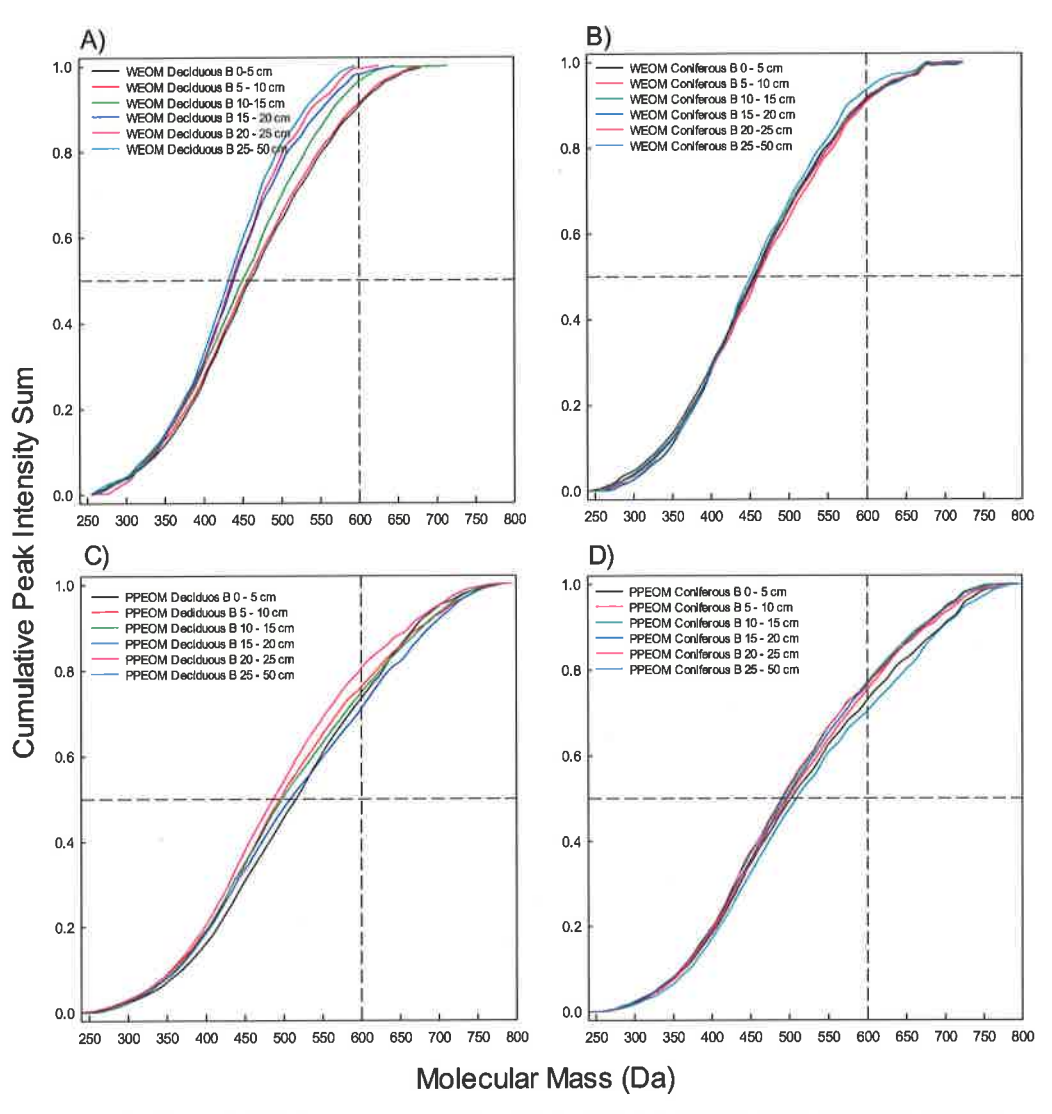


Fig. 3. Molecular mass intensity profiles binned into 10-Da increments between 220 and 800 Da plotted as a cumulative fraction function for the aromatic SOM components of the deciduous and coniferous 0-5 cm to 25-50 cm B horizon soil increments.

adsorption taking place through oxygen-containing functional groups leading to a lower O/C ratio for the remaining WEOM molecules. The changes for the unique coniferous WEOM are much smaller in magnitude as compared with the changes in the deciduous WEOM, suggesting

much less adsorptive-driven fractionation as the WEOM is transported down the soil profile.

Table 4

The average molecular formula, mass, H/C ratio, O/C ratio, and modified aromaticity index for the WEOM PPEOM marker molecules unique to the 0–10, 10–20, and 20–50 cm soil depths in the deciduous and coniferous forest stands.

Soil	Depth	Formula	m/z	H/C	O/C	AI_{mod}
WEOM						
Deciduous	Unique 0-10 cm	C _{23.8} H _{27.8} O _{10.0} N _{1.1} S _{0.4}	500.9	1.19	0.43	0.25
	Unique 10-20 cm	C _{23.8} H _{30.4} O _{9.2} N _{1.2} S _{0.4}	493.0	1.31	0.39	0.16
	Unique 20-50 cm	C _{23.8} H _{27.8} O _{8.5} N _{1.2} S _{0.4}	482.6	1.38	0.37	0.15
Coniferous	Unique 0-10 cm	C24.8H30.7O9.6N1.4S0.4P0.01	514.8	1.26	0.40	0.19
	Unique 10-20 cm	C24.6H30.6O9.6N1.3S0.4P0.02	510.3	1.27	0.41	0.19
	Unique 20-50 cm	$C_{25.0}H_{32.4}O_{9.3}N_{1.4}S_{0.5}P_{0.01}$	514.3	1.33	0.39	0.17
PPEOM						
Deciduous	Unique 0-10 cm	$C_{30,1}H_{23,3}O_{9,4}N_{1,3}S_{0,9}P_{0,53}$	596.6	0.83	0.35	0.53
	Unique 10-20 cm	C31.2H24.3O9.4N1.6S0.9P0.42	611.7	0.85	0.34	0.50
	Unique 20-50 cm	C _{30.6} H _{24.3} O _{10.0} N _{1.3} S _{0.8} P _{0.38}	604.2	0.85	0.36	0.49
Coniferous	Unique 0–10 cm	C _{30.9} H _{23.2} O _{9.8} N _{1.6} S _{1.1} P _{0.47}	621.4	0.80	0.36	0.56
	Unique 10–20 cm	C31.3H22.5O10.6N1.4S0.8P0.34	620.3	0.77	0.39	0.54
	Unique 20-50 cm	$C_{30.1}H_{24.9}O_{9.6}N_{1,2}S_{0.8}P_{0.039}$	593.1	0.89	0.36	0.49

T. Ohno et al. Geoderma 308 (2017) 1-8

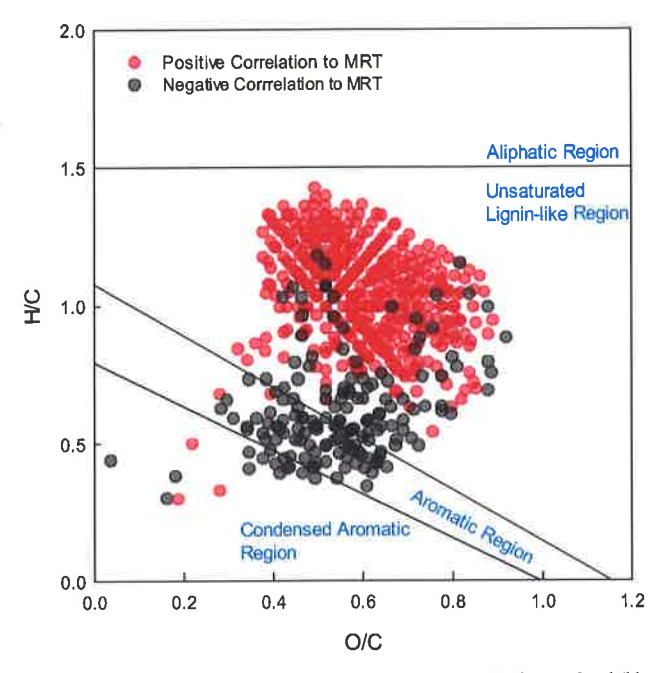


Fig. 4. van Krevelen plots of the assigned formulas that are positively correlated (blue symbols) and negatively correlated (orange symbols) to $^{14}\mathrm{C}$ mean residence time of the B horizon soil organic matter. The p=0.05 level was used as the significance level for the correlations. (For interpretation of the references to colour in this figure legend, the reader is referred to the web version of this article.)

3.5. FT-ICR-MS characterization of PPEOM

The unique PPEOM molecular markers indicate that the adsorbed molecules have much higher aromaticity as compared with the WEOM molecular markers (Table 4). Unlike the results for the deciduous WEOM data, there were only minor changes in the chemical properties of the deciduous PPEOM with increasing depth. In addition, the cumulative sum distributions were similar between the deciduous and coniferous profiles (Fig. 3C & D). To explore the relationship between B horizon MRT and PPEOM chemical composition as determined by FT-ICR-MS, a correlation-based technique (Singer et al., 2012; Stubbins et al., 2014; Chassé et al., 2015) was used to relate the normalized intensity of assigned formulas present in all six of the B horizon samples from both forest types to the SOM MRT (Fig. 4). The red symbols are positively correlated to MRT (longer MRT), and the black symbols are negatively correlated to SOM MRT (shorter MRT). The SOM molecules with H/C > 0.8 were predominately correlated with slower processing or longer radiocarbon MRT, while more aromatic compounds were correlated with faster processing (shorter MRT). The longer MRT, positively correlated components consisted of 16% aromatic and 84% highly unsaturated/lignin-like molecules as compared with the shorter MRT, negatively correlated components, which were 87% aromatic and 12% unsaturated/lignin-like molecules. The dominance of the highly unsaturated/lignin-like PPEOM molecules in the pool correlated with longer MRT may be due to low demand for these adsorbed compounds to serve as an energy source for microbes. Another explanation could be the traditional viewpoint that lignin-type molecules are recalcitrant due to their inherent aromatic structures and that the chemical composition of the molecules are critical factors for their long MRT in the soil.

Classically, aromatic SOM molecules have been viewed as a highly recalcitrant component of plant biomass due to its high aromaticity. In addition, it has been thought that lignins are transformed stepwise in microbial-driven processes to phenolic aldehydes and then to quinones which undergo polymerization reactions and conversion to high molecular weight soil organic matter molecules (Sparks, 2003). However, recent studies have shown that plant biomass lignin undergoes

decomposition in the presence of available C energy sources suggesting that lignin does not have inherent chemical recalcitrance (Dignac et al., 2005; Heim and Schmidt, 2007; Klotzbücher et al., 2011). These findings, in part, have informed current thinking about soil organic matter as a continuum of smaller biomolecules stabilized by its interaction with mineral surfaces (Schmidt et al., 2011; Lehmann and Kleber, 2015).

4. Conclusions

Our study provides a characterization of the SOM ¹⁴C abundance, thermal properties, and chemical composition of the WEOM and PPEOM fractions of SOM as a function of soil depth in pedons developed under deciduous and coniferous forest types. We found that ¹⁴C abundance was enriched for the SOM developed under a coniferous forest type as compared with development under a deciduous forest type, suggesting an overall shorter average MRT in subsoils under conifers. Ultrahigh resolution mass spectrometry data suggest that under both forest types the aromatic-type components of SOM are negatively correlated to mean residence time and the highly unsaturated, lignin-like components are positively correlated to MRT. Calculations show that the loading rate of amorphous and poorly-crystalline Fe and Al mineral-bound C is not statistically different in the two forest type soils. We suggest that the sorptive stabilization has reached saturation in the coniferous forest soils allowing younger SOM to be transported deeper in the soil, resulting in the observed younger radiocarbon MRT in the coniferous forest type. The findings here are important for understanding how the global C cycle may be affected by climate-driven shifts in forest composition (Iverson et al., 2008), and how we interpret our measurements of total C in forest soils. Shifting species composition in forests is likely to affect the stability of soil C, and understanding these processes will be critical for the effective management of ecosystem services in a future changing climate.

Acknowledgements

Radiocarbon analysis was supported by the Radiocarbon Collaborative, which is jointly sponsored by the USDA Forest Service, Lawrence Livermore National Laboratory, and Michigan Technological University. This project was supported by USDA-NIFA-AFRI-2013-67019-21368 and the Maine Agricultural and Forest Experiment Station Hatch Project MEO-H-1-00472-11. This is MAFES Journal no. 3552.

Appendix A. Supplementary data

Supplementary data to this article can be found online at http://dx.doi.org/10.1016/j.geoderma.2017.08.023.

References

Ahrens, B., Braakhekke, M.C., Guggenberger, G., Schrumph, M., Reichstein, M., 2015. Contribution of sorption, DOC transport and microbial interactions to the ¹⁴C age of a soil organic carbon profile: insights from a calibrated process mode. Soil Biol. Biochem. 88, 390–402.

Chassé, A.W., Ohno, T., 2016. Higher molecular mass organic matter molecules compete with orthophosphate for adsorption to iron (oxy)hydroxide. Environ. Sci. Technol. 50, 7461-7469.

Chassé, A.W., Ohno, T., Higgins, S.R., Amirbahman, A., Yildirim, N., Parr, T.B., 2015. Chemical force spectroscopy evidence supporting the layer-by-layer model of organic matter binding to iron (oxy)hydroxide mineral surfaces. Environ. Sci. Technol. 49, 9733-9741.

Davis, J.C., Proctor, I.D., Southon, J.R., Caffee, M.W., Heikkinen, D.W., Roberts, M.L., Moore, T.L., Turteltaub, K.W., Nelson, D.E., Loyd, D.H., Vogel, J.S., 1990. LLNL/US AMS facility and research program. Nucl. Instrum. Meth. B 52, 269–272.

Dignac, M.-F., Bahri, H., Rumpel, C., Rasse, D.P., Bardoux, G., Balesdent, J., Girardin, C., Chenu, C., Mariotti, A., 2005. Carbon-13 natural abundance as a tool to study the dynamics of lignin monomers in soil: an appraisal at the Closeaux experimental field (France). Gerderma 128, 3–17.

Dittmar, T., Koch, B., Hertkorn, N., Kattner, G., 2008. A simple and efficient method for the solid-phase extraction of dissolved organic matter (SPE-DOM) from seawater. Limnol, Oceanogr, Methods 6, 230-235,

Biol. Biochem. 52, 29-32.

- Fernandez, I., Rustad, L., David, M., Nadelhoffer, K., Mitchell, M., 1999. Mineral soil and solution responses to experimental N and S enrichment at the Bear Brook Watershed in Maine (BBWM). Environ. Monit. Assess. 55, 165-185.
- Fernández, J.M., Peltre, C., Craine, J.M., Plante, A.F., 2012. Improved characterization of soil organic matter by thermal analysis using CO₂/H₂O evolved gas analysis. Environ, Sci. Technol. 46, 8921-8927.
- Heim, A., Schmidt, M.W.I., 2007. Lignin turnover in arable soil and grassland analyzed with two different labelling approaches. Eur. J. Soil Sci. 58, 599-608.
- Iverson, L.R., Prasad, A.M., Matthews, S.N., Peters, M., 2008. Estimating potential habitat for 134 eastern US tree species under six climate scenarios. For. Ecol. Manag. 254, 390-406.
- lyengar, S.S., Zelazny, L.W., Martens, D.C., 1994. Effect of photolytic oxalate treatment
- on soil hydroxyl-interlayed vermiculites. Clay Clay Miner. 29, 429-434. Kaiser, K., Kalbitz, K., 2012. Cycling downwards - dissolved organic matter in soils. Soil
- Karathanasis, A.D., Harris, W.G., 1994. Quantitative thermal analysis of soil materials. In: Amonette, J.E., Zelazny, L.W. (Eds.), Quantitative Methods in Soil Mineralogy. Soil Science Society of America, Madison WI, pp. 360-411.
- Klotzbücher, T., Filley, T.R., Kaiser, K., Kalbitz, K., 2011. A study of lignin degradation in leaf and needle litter using 13C-labelled tetramethylammonium hydroxide (THAM) thermochemolysis: comparison with CuO oxidation and van Soest methods. Org. Geochem. 42, 1271-1278.
- Koch, B.P., Dittmar, T., 2006. From mass to structure: an aromaticity index for highresolution mass data of natural organic matter. Rapid Commun. Mass Spectrom. 20,
- Kujawinski, E.B., Behn, M.D., 2006. Automated analysis of electrospray ionization Fourier-transform ion cyclotron resonance mass spectra of natural organic matter. Anal. Chem. 78, 4363-4373.
- Lehmann, J., Kleber, M., 2015. The contentious nature of soil organic matter. Nature 528, 60-68.
- Mathieu, J.A., Hatté, C., Balesdent, J., Parent, E., 2015. Deep soil carbon dynamics are driven more by soil type than by climate: a worldwide meta-analysis of radiocarbon profiles. Glob. Chang. Biol. 21, 4278–4292.
- Minderman, G., 1968. Addition, decomposition and accumulation of organic matter in forests, J. Ecol. 56, 355-362.
- Norton, S.A., 1999. The Bear Brook Watershed in Maine: A Paired waterhed experiment: The First Decade (1987-1999). (Springer Netherlands).
- Norton, S., Kahl, J., Fernandez, I., Haines, T., Rustad, L., Nodvin, S., Scofield, J., Strickland, T., Erickson, H., Wigington, P., Lee, J., 1999. The Bear Brook Watershed, Maine (BBWM), USA. Environ. Monit. Assess. 55, 7-51.
- Ohno, T., Ohno, P.E., 2013. Influence of heteroatom pre-selection on the molecular formula assignment of soil organic matter components determined by ultrahigh resolution mass spectrometry. Anal. Bioanal. Chem. 405, 3299-3306.
- Ohno, T., Parr, T.B., Gruselle, M.-C.I., Fernandez, I.J., Sleighter, R.L., Hatcher, P.G., 2014. Molecular composition and biodegradability of soil organic matter: a case study comparing two New England forest types. Environ. Sci. Technol. 48, 7229-7236.
- Pansu, M., Gautheyrou, J., 2006. Mineralogical separation by selective dissolution. In: Pansu, M., Gautheyrou, J. (Eds.), Handbook of Soil Analysis: Mineralogical. Organic and Inorganic Methods. Springer Science & Business Media, Berlin, pp. 167-219.
- Peltre, C., Fernández, J.M., Craine, J.M., Plante, A., 2013. Relationships between biological and thermal indices of soil organic matter stability differ with soil organic

- carbon level. Soil Sci. Soc. Am. J. 77, 2020-2028.
- Plante, A.F., Fernández, J.M., Haddix, M.L., Steinweg, J.M., Conant, R.T., 2011. Biological, chemical and thermal indices of soil organic matter stability in four grassland soils. Soil Biol. Biochem. 43, 1051-1058.
- Rovira, P., Kurz-Besson, C., Coûteaux, M.-M., Vallejo, V.R., 2008. Changes in litter properties during decomposition: a study by differential thermogravimetry and scanning calorimetry. Soil Biol. Biochem. 40, 172-185.
- SanClements, M.D., Fernandez, I.J., Norton, S.A., 2010. Soil chemical and physical properties at the Bear Brook Watershed in Maine, USA. Environ. Monit. Assess. 171, 111-128.
- Scharlemann, J.P.W., Tanner, E.V.J., Hiederer, R., Kapos, V., 2014. Global soil carbon: understand and managing the largest terrestrial carbon pool. Carbon Manage. 5,
- Schmidt, M.W.I., Torn, M.S., Abiven, S., Dittmar, T., Guggenberger, G., Janssens, I.A., Kleber, M., Kögel-Knabner, I., Lehmann, J., Manning, D.A.C., Nannipieri, P., Rasse, D.P., Weiner, S., Trumbore, S.E., 2011. Persistence of soil organic matter as an ecosystem property. Nature 478, 49-56.
- Schnitzer, M., Schuppli, P., 1989. Methods for the sequential extraction of organic-matter from soils and soil fractions. Soil Sci. Soc. Am. J. 53, 1418-1424.
- Seidel, M., Beck, M., Riedel, T., Waska, H., Suryaputra, I.G.N.A., Schnetger, B., Niggemann, J., Simon, M., Dittmar, T., 2014. Biogeochemistry of dissolved organic matter in an anoxic intertidal creek bank. Geochim. Cosmochim. Acta 140, 418-434.
- Singer, G.A., Fasching, C., Wilhelm, L., Niggemann, J., Steier, P., Dittmar, T., Battin, T.J., 2012. Biogeochemically diverse organic matter in alpine glaciers and its downstream fate. Nat. Geosci. 5, 710-714.
- Sleighter, R.L., Hatcher, P.G., 2007. The application of electrospray ionization coupled to ultrahigh resolution mass spectrometry for the molecular characterization of natural organic matter. J. Mass Spectrom. 42, 559-574.
- Song, X., Boily, J.-F., 2016. Surface and bulk thermal dehydroxylation of FeOOH polymorphs. J. Phys. Chem. A 120, 6249-6257.
- Sparks, D.L., 2003. Environmental Soil Chemistry, 2nd Ed. Academic Press, New York. Stubbins, A., Lapierre, J.-F., Berggren, M., Prairie, Y.T., Dittmar, T., del Giorgio, P.A., 2014. What's in an EEM? Molecular signatures associated with dissolved organic fluorescence in boreal Canada. Environ. Sci. Technol. 48, 10598–10606. Stuiver, M., Polach, H.A., 1977. Discussion: reporting of ¹⁴C data. Radiocarbon 19,
- 355-363.
- Torn, M.S., Swanston, C.W., Castanha, C., Trumbore, S., 2009. Storage and turnover of organic matter in soil. In: Huang, P.M., Senesi, N. (Eds.), Biophysico-chemical Processes Involving Natural Nonliving Organic Matter in Environmental Systems. Wiley, Hoboken, pp. 219-272.
- Trumbore, S.E., 1993. Comparison of carbon dynamics in tropical and temperature soils using radiocarbon measurements. Glob. Biogeochem. Cycles 7, 275–290.
 Trumbore, S.E., Vogel, J.S., Southon, J.R., 1989. AMS ¹⁴C measurements of fractionated
- soil organic matter: an approach to deciphering the soil carbon cycle. Radiocarbon 31, 644–654.
- Vogel, J.S., Southon, J.R., Nelson, D.E., 1987. Catalyst and binder effects in the use of filamentous graphite for AMS. Nucl. Instrum. Meth. B. 29, 50-56.
- Wagai, R., Mayer, L.M., Kiayama, K., Shirato, Y., 2013. Association of organic matter with iron and aluminum across a range of soils determined via selective dissolution techniques coupled with dissolved nitrogen analysis. Biogechemistry 112, 95-109.
- Zsolnay, A., 2003. Dissolved organic matter: artefacts, definitions, and functions. Geoderma 113, 187-209.

Supplementary Material

¹⁴C Mean Residence Time and Its Relationship with Thermal Stability and Molecular Composition of Soil Organic Matter: A Case Study of Deciduous and Coniferous Forest Types

Tsutomu Ohnoa*, Katherine A. Heckmanb, Alain F. Plantec, Ivan J. Fernandezd, Thomas B. Parr e

- ^a School of Food and Agriculture, University of Maine, Orono, Maine 04469, USA
- ^b USDA Forest Service, Northern Research Station, Houghton, MI 49931, USA
- Department of Earth and Environmental Sciences, University of Pennsylvania, Philadelphia,
 Pennsylvania 19104, USA
- d School of Forest Resources, University of Maine, Orono, Maine 04469, USA
- e Department of Biology, University of Oklahoma, Norman, Oklahoma 73019, USA
- * Corresponding author: Tel.: +1 207 581 2975; E-mail address: ohno@maine.edu

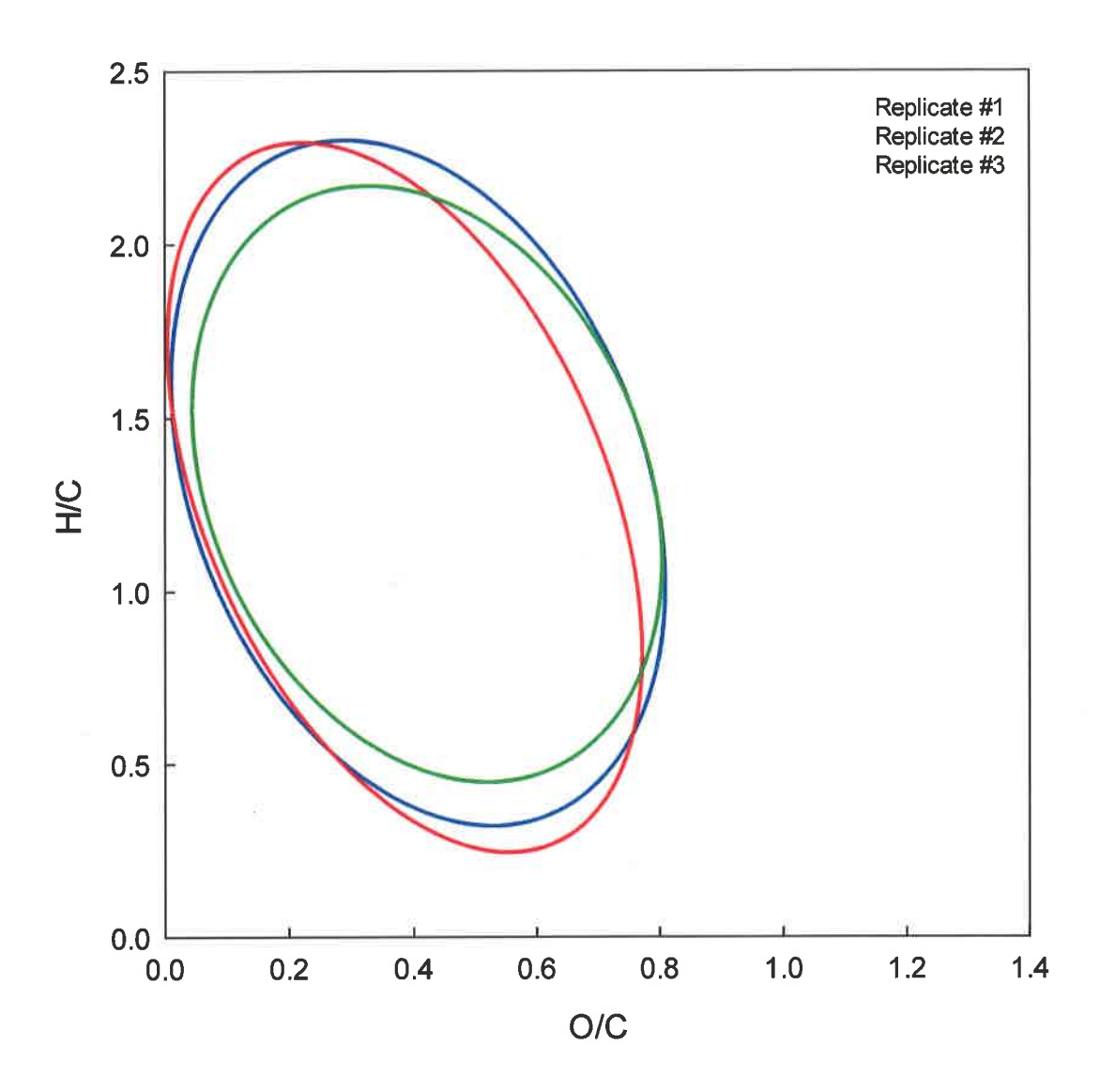


Fig. S1. van Krevelen diagram of the water-extractable organic matter 0-5 cm B-horizon soil isolated from three replicate sampling locations in the BBWM deciduous forest type stand. The replicate samples used were from a 2006 sampling campaign at BBWM. For clarity of display, only 500 randomly selected data points are shown for each of the replicates. The 95% confidence ellipses are based on the complete data set for each replicate.

Supplementary Fig. S2

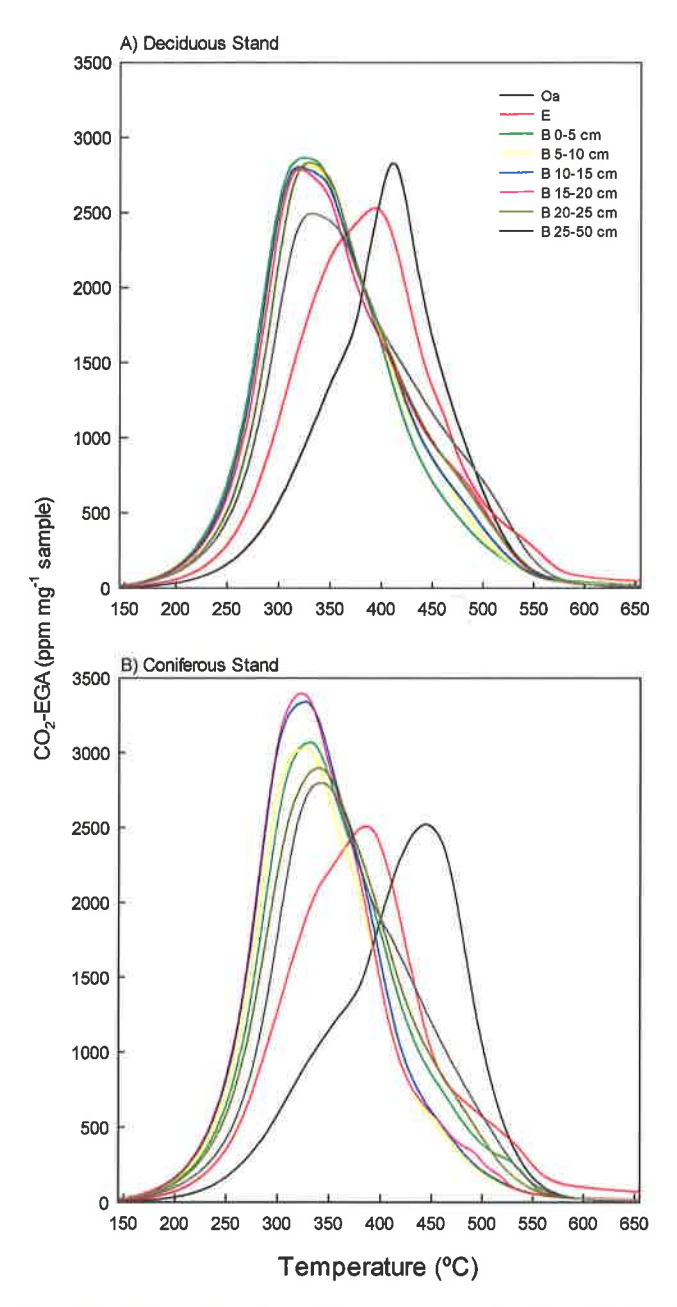


Fig. S2. CO_2 evolved gas thermograms for the (A) deciduous and (B) coniferous O_a , E, and B horizon soil samples.